Immunocytochemical localization of S100A1 in mitochondria on cryosections of the rat heart

A. Brezová[1], C. W. Heizmann[2] and B. Uhrík[1]

[1] *Institute of Molecular Physiology and Genetics, Slovak Academy of Sciences, Vlárska 5, Bratislava, Slovakia*
[2] *Division of Clinical Chemistry and Biochemistry, Department of Pediatrics, University of Zurich, Steinwiesstrasse 75, 8032 Zurich, Switzerland*

Abstract. Immunocytochemical localization studies of S100A1 in muscle cells have so far yielded variable and conflicting results mainly due to different sample preparation techniques for immunoelectron microscopy. To minimize denaturation by fixation and embedding, cryofixation and cryosectioning followed by immunolabelling were used in the present study. Rat hearts were gently prefixed in a mixture of paraformaldehyde and glutaraldehyde. Samples from left and right ventricles and left and right atria were cryoprotected by sucrose and shock-frozen in liquid nitrogen. Ultrathin cryosections were labelled with rabbit polyclonal antiserum against S100A1. The sections were then incubated with secondary antibody conjugated to FITC (for fluorescence microscopy) or with protein A conjugated to 5 nm gold particles (for electron microscopy). The most prominent sites immunolabelled for S100A1 were mitochondria. In the fluorescence microscope the labelling of mitochondria was intense, suppressing the labelling in other compartments. In accordance with previous studies labelling of sarcoplasmic reticulum, Z-lines, actin and myosin filaments could also be detected in the electron microscope.

Key words: Ca^{2+}-binding proteins — S100A1 — Heart muscle — Cryosections — Mitochondria

Introduction

The regulation of a great number of cellular processes depends on calcium. Calcium binding proteins represent an important link between the Ca^{2+} signal and corresponding effectors in the cellular machinery. S100A1 is a member of the family of S100 proteins, the largest subgroup of EF-hand Ca^{2+}-binding proteins (for a review see Marenholz et al. 2004; Heizmann et al. 2007). It is expressed predominantly in heart muscle cells and slow-twitch skeletal muscle fibers, and several studies have invoked its role at various stages of the contraction-relaxation cycle (Adhikari and Wang 2001; Yamasaki et al. 2001; Kiewitz et al. 2003; Most et al. 2005).

The search for target proteins of S100A1 and immunocytochemical localization studies have resulted in suggesting a number of cellular sites and compartments where S100A1 could exert its function and take part in signal transfer (Heierhorst et al. 1996; Ivanenkov et al. 1996; Treves et al. 1997; Mandinova et al. 1998). In particular, sarcoplasmic reticulum (SR) and myofibrils at different levels of the sarcomere, with the highest density at Z-lines, were found to have numerous binding sites for anti-S100A1 antibodies (Maco et al. 2001). These localizations correspond well with the sites of known target proteins for S100A1. However, other structures, like mitochondria, nuclei, sarcolemma or intercalated discs were also S100A1-positive occasionally.

The extent and distribution of immunolabelling is dependent on the method of tissue preparation, which must be considered when comparing results from different laboratories. Haimoto and Kato (1987, 1988) studied the ultrastructural localization of S100A1 in mouse slow-twitch skeletal and heart muscle cells using the post-embedding peroxidase-labelled antibody method. After periodate-lysine-paraformaldehyde prefixation and embedding into OCT, 6-μm-thick cryostat-cut sections were treated with HRP-labeled antibody, fixed with glutaraldehyde, incubated in diaminobenzidine and hydrogen peroxide, postfixed in

Correspondence to: Branislav Uhrík, Institute of Molecular Physiology and Genetics, Slovak Academy of Sciences, Vlárska 5, 833 34 Bratislava 37, Slovakia
E-mail: branislav.uhrik@savba.sk

osmium tetroxide, dehydrated and embedded in Epon 812. In slow-twitch muscle cells, this treatment resulted in the occasional presence of fine granular deposits on the outer mitochondrial membrane, but not within the mitochondria. Most deposits were found on polysomes in interfibrillar spaces, SR, the plasma membrane and thick and thin filaments. In heart muscle cells, no labelling of mitochondria was described. The deposits were densely localized on the polysomes, Z-line, fascia adherens of intercalated discs and in the lumen of junctional SR. Labelling of thick and thin filaments and nuclei was also present.

A different image of S100A1-labelling appeared in studies using pre-embedding immunogold cytochemistry on rat heart and leg muscles (Donato et al. 1989) and post-embedding (Epon-Araldite) immunogold cytochemistry on avian skeletal muscles (Arcuri et al. 2002). In rat cardiac and skeletal cells, immunogold was found at sarcolemmal membranes, the SR membranes, T-tubules, the outer mitochondrial membrane, and in the adjacent sarcoplasm. No association with nuclei or with myofibrils was observed. In avian skeletal muscles, immunogold was detected only at the sarcolemma, SR and T-tubules.

Another post-embedding immunogold study was performed on human heart atrium and labelling of mitochondria was only marginally mentioned. Following fixation in a glutaraldehyde/paraformaldehyde mixture, the specimens were dehydrated in ethanol and embedded in a low viscosity Lowicryl K4M medium and polymerized at –40°C (Maco et al. 2001). In contrast to the Epon-Araldite mixture, Lowicryl K4M is hydrophilic. The labelling of mitochondria was uniform on the whole section area and its density was comparable to the immunogold density over I-bands. The most intensive labelling was found on Z-lines and sarcoplasmic reticulum.

The discrepancies in localization of S100A1 in mitochondria and also in other subcellular compartments have prompted us to use a methodical approach, which preserves cells in a more gentle way avoiding denaturing effects of dehydration and embedding in plastic media, and allowing a simultaneous labelling of all cellular components in contrast to pre-embedding immunocytochemistry or post-embedding in OCT, where the reagents have to diffuse across semi-thick sections to reach the target structures. We have used ultrathin cryosections for immunolabelling. In the present paper we show, that mitochondria in rat cardiac cells are the structure most densely labelled with anti-S100A1 antibodies. The main results of this study have been reported and published in abstracts (Brezová et al. 2001, 2002).

Materials and Methods

All experiments were performed according to institutional guidelines and were approved by the local ethical committee.

Preparation of rat heart tissue blocks

Male Wistar rats with body weights of 200–250 g, standard pellet diet and tap water *ad libitum*, were decapitated. Their hearts were quickly dissected, cannulated through aorta and perfused for 15 min with a modified Krebs–Henseleit solution (pH 7.4) at 37 °C, (in mmol/l): 118.0 NaCl, 27.2 $NaHCO_3$, 1.2 $MgSO_4$, 1.0 KH_2PO_4, 1.59 $CaCl_2$, 3.0 KCl, 11.1 glucose, gassed with 95% O_2 and 5% CO_2. The hearts of four animals were subsequently fixed by perfusion with a mixture of 1% formaldehyde and 0.025% glutaraldehyde in 0.1 mol/l phosphate buffer (PBS), pH 7.4, for 15 – 20 min. Samples from left and right atria and ventricles were dissected and postfixed for 3 – 4 h in the same solution. After short washing with 0.1 mol/l PBS, the samples were cut into blocks of < 1 mm^3 and incubated overnight at room temperature in 2.2 mol/l sucrose in 0.1 mol/l PBS in a wet chamber (Tokuyasu 1986). On the next day, the sucrose-infused tissue blocks were placed on aluminium pins and frozen in liquid nitrogen.

Ultrathin cryosections

Ultrathin (150 nm) cryosections were made with a 35° cryo diamond knife (Diatome) on a Reichert Ultracut E ultramicrotome equipped with an FC 4D cryoattachment at about –100 °C. Cryosections were retrieved from the cryochamber with a copper loop containing 2.2 mol/l sucrose and 0.75% gelatin in HEPES buffered saline (HBS) (in mmol/l: 10 HEPES, 150 NaCl, 1.2 $CaCl_2$, 20 NaN_3) at pH 7.5. Thawed sections were transferred onto polylysinated coverslips (thickness 1) for fluorescent microscopy (FM) or onto 50 square mesh nickel grids supported with formvar film for electron microscopy (EM).

Immunolabelling

Sections on cover glasses (FM) or grids (EM) were washed and preincubated in 0.02 mol/l glycine in 0.01 mol/l HBS overnight to quench remaining reactive aldehyde groups. Then they were incubated in a blocking solution (BS = 0.5% bovine serum albumin, 0.02 mol/l glycine in 0.01 mol/l HBS) for 7 min. Subsequent immunolabelling of S100A1 was performed with rabbit polyclonal antiserum against S100A1 (diluted 1:100 in BS) for 2 hours. Purified polyclonal antiserum was obtained by immunization of rabbits with recombinant human S100A1 produced in E. coli cultures (Ilg et al. 1996). These polyclonal antibodies are specific and do not cross-react with other S100 or Ca^{2+}-binding proteins or with other cellular proteins.

Cover glasses or grids were washed with 0.02 mol/l glycine in 0.01 mol/l HBS for 45 min and with BS for 7 min. Sections for FM on cover glasses were incubated in goat

anti-rabbit IgG conjugated with FITC (SIGMA, No. F-9887, diluted 1:200) for 30 min. Sections for EM on grids were incubated with protein A conjugated to 5 nm gold particles (British BioCell International) diluted 1:10 in BS for 30 min. Cover glasses or grids were washed in 0.02 mol/l glycine in 0.01 mol/l HBS for 10 min and then in 0.01 mol/l HBS for 10 min.

The cover glasses were then mounted on glass slides using small drops of a mounting medium (90% glycerol in 0.01 mol/l HBS with 0.1 g/ml DABCO).

The grids were fixed with drops of 1% glutaraldehyde in 0.1 mol/l HEPES (pH 7.1) for 5 min, washed shortly with 0.1 M HEPES and with deionized water. Silver enhancement was then performed according to the neutral pH silver development method by Lah et al. (1990).

Then the grids were placed on drops of embedding solution (1:1 fresh mixture of 4% 25 centipoise methyl cellulose and 2% uranyl acetate) for 10 min and looped out with a ≈ 3.5 mm diameter copper loop, disposed of excess fluid by touching the surface of a filter paper, left to dry and loosened.

All incubations were performed in a wet chamber.

The specificity of immunolabelling was verified by omitting primary antibodies during the labelling procedure or by mixing primary antibodies with the antigen prior to labelling.

Microscopy

The sections were examined under an electron microscope JEOL JEM 1200 EX at 80 kV or under a fluorescent microscope (Axioskop, Opton) using an immersion objective with 100× magnification.

Results

Fluorescent microscopy

Subcellular localization of S100A1 was first determined using fluorescent imaging. Fig. 1 shows longitudinally sectioned cardiac cells from the left (A) and right (B) ventricles. Fluorescent structures are arranged into parallel strips of luminous beads running along the full length of the section without any indication of myofibrillar striations. Such an arrangement suggests that the bright structures labelled for S100A1 are situated in intermyofibrillar spaces.

Immunolabelling in atrial cells was similar. In oblique (Fig. 2A) or transverse (Fig. 2B) sections the fluorescent structures changed their orientation or appeared as isolated spots.

In control specimens the labelling disappeared. Fig. 3 shows the cells from the left ventricle treated by primary antibodies mixed with the antigen prior to labelling.

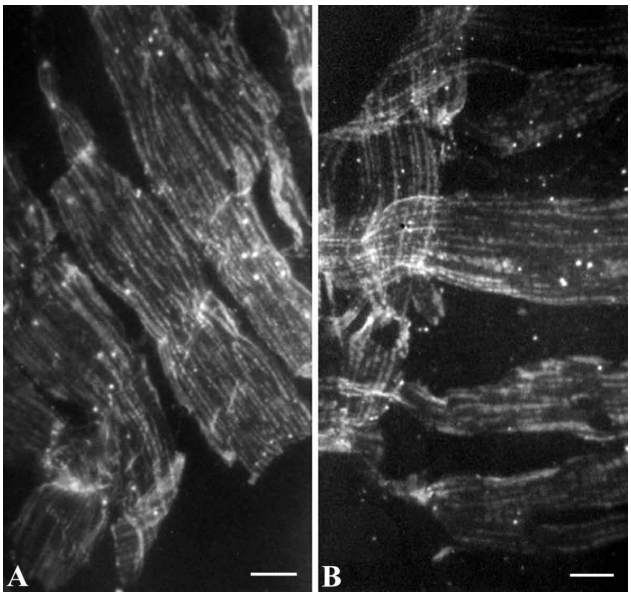

Figure 1. Immunolabelling of S100A1 in longitudinal sections of rat cardiac cells from the left ventricle **(A)** and from the right ventricle **(B)** in FM. *Bars:* 10 μm

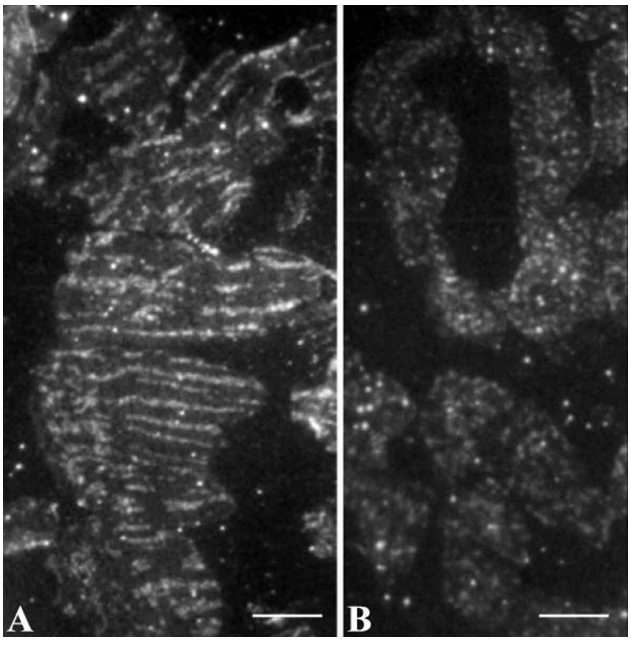

Figure 2. Immunolabelling of S100A1 in sections of rat cardiac cells from the left atrium **(A)** and from the right atrium **(B)** in FM. *Bars:* 10 μm

Electron microscopy

Immunocytochemical localization of S100A1 at the ultrastructural level showed a predominant labelling of mito-

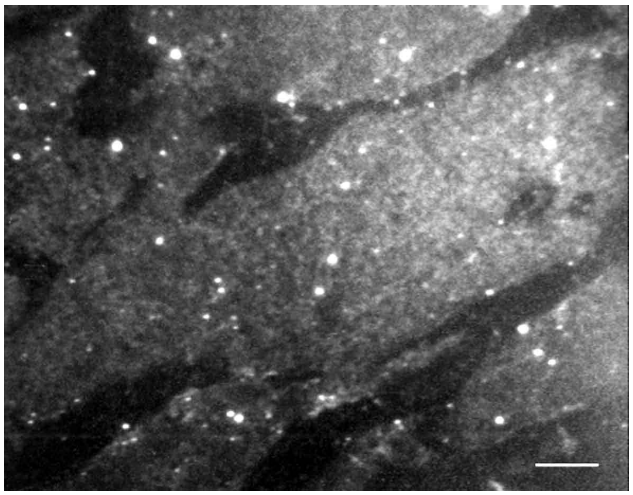

Figure 3. Control specimen in FM. Cells from the left ventricle were treated by primary antibodies mixed with the antigen prior to labelling. *Bar:* 10 μm

chondria as demonstrated in a longitudinal section of a rat cardiac cell from the left ventricle (Fig. 4). In addition to mitochondria, the silver-enhanced gold particles could be found in elements of sarcoplasmic reticulum (arrowheads) and in myofibrils at different levels of the sarcomere. Similar labelling was seen in cells from the right ventricle as shown in Fig. 5 at a higher magnification.

Immunolabelling in atrial cells confirmed mitochondria as the site with the highest prevalence of gold particles (Fig. 6 A, B). Natriuretic granules in the right atrium remained unstained (Fig. 6 B).

In control specimens the labelling was only sporadic without preference to any structural component. Fig. 7 shows a cell from the left ventricle treated by primary antibodies mixed with the antigen prior to labelling.

Discussion

The main results of this study not only confirm the presence of S100A1 in mitochondria, but show clearly that these organelles are the site with the highest density of immunogold particles. The particles are localized over the whole cross-sectional area of all mitochondria and not only occasionally at their periphery as shown by Haimoto and Kato (1987, 1988) and Donato et al. (1989). Evidently, little or no denaturation and a simultaneous labelling of all cellular components as ensured only by cryofixation and cryosectioning may be crucial for immunolabelling of some antigens and for their detection in some compartments. In contrast to our present observations, the labelling of mitochondria

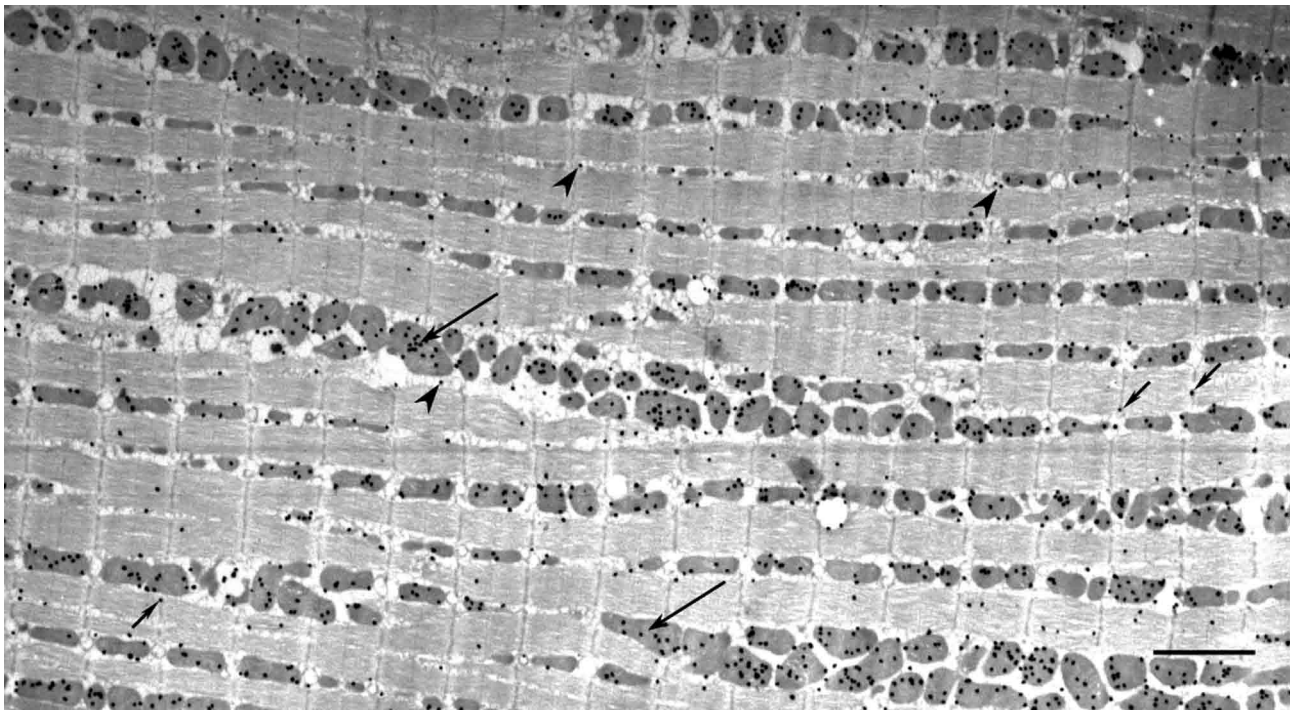

Figure 4. Immunolabelling of S100A1 in the longitudinal section of a rat cardiac cell from the left ventricle in EM. Large arrows – mitochondria; *small arrows* – labelling at Z-lines; *arrowheads* – labelling at sarcoplasmic reticulum. *Bar*: 2.5 μm

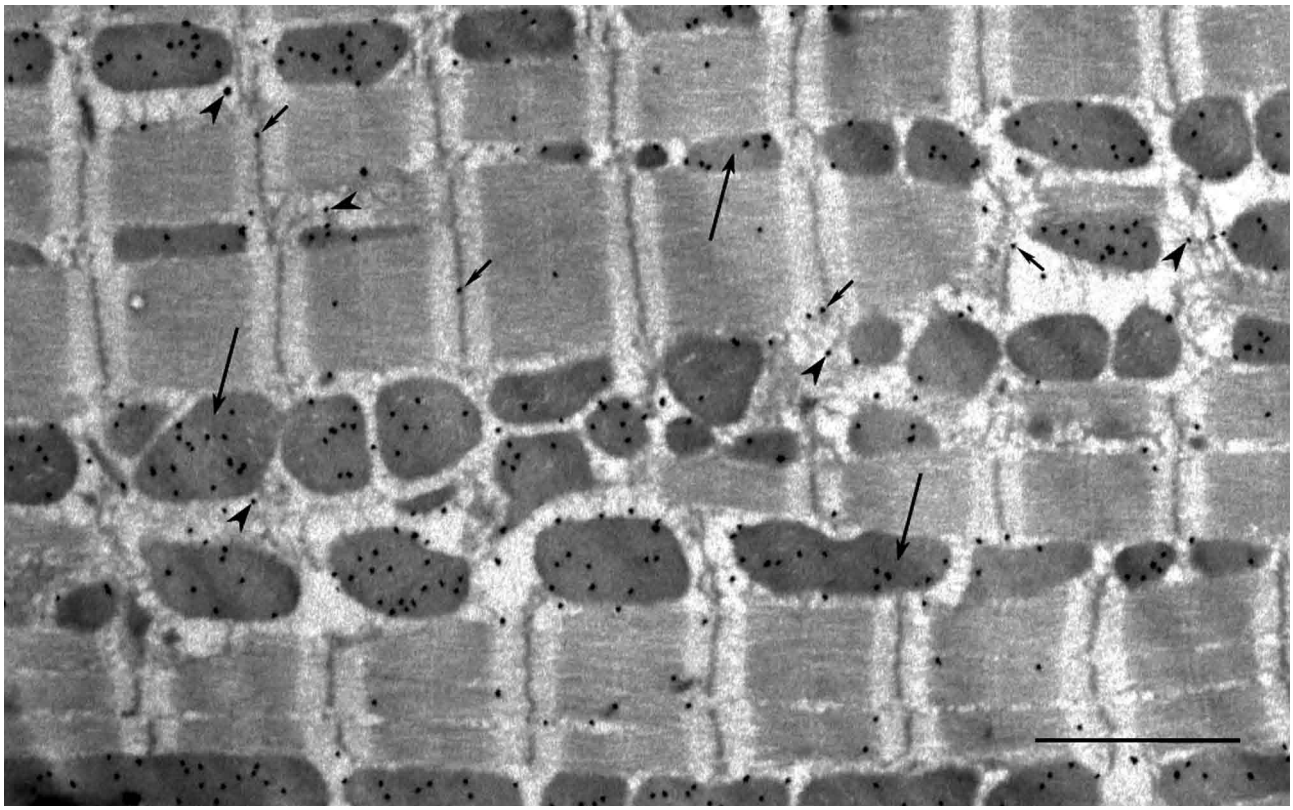

Figure 5. Immunolabelling of S100A1 in the longitudinal section of a rat cardiac cell from the right ventricle in EM. *Large arrows* – mitochondria; *small arrows* – labelling at Z-lines; *arrowheads* – labelling at sarcoplasmic reticulum. *Bar*: 2.5 μm

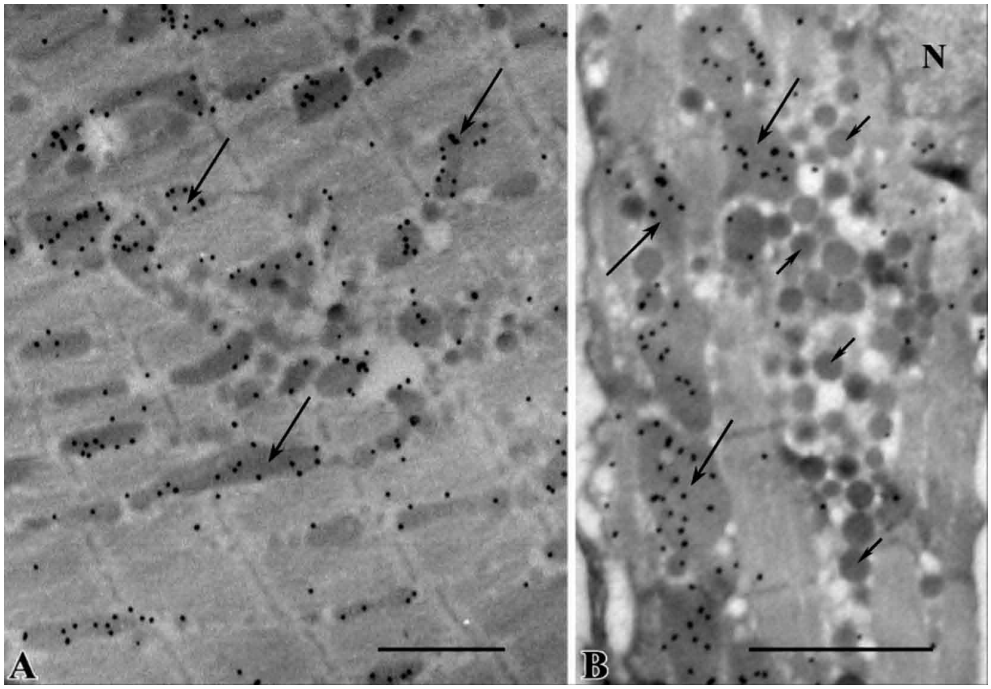

Figure 6. Immunolabelling of S100A1 in sections of rat cardiac cells from the left atrium **(A)** and from the right atrium **(B)** in EM. *Large arrows* – mitochondria; *small arrows* – atrial natriuretic granules; *N* – nucleus. *Bars*: 2 μm

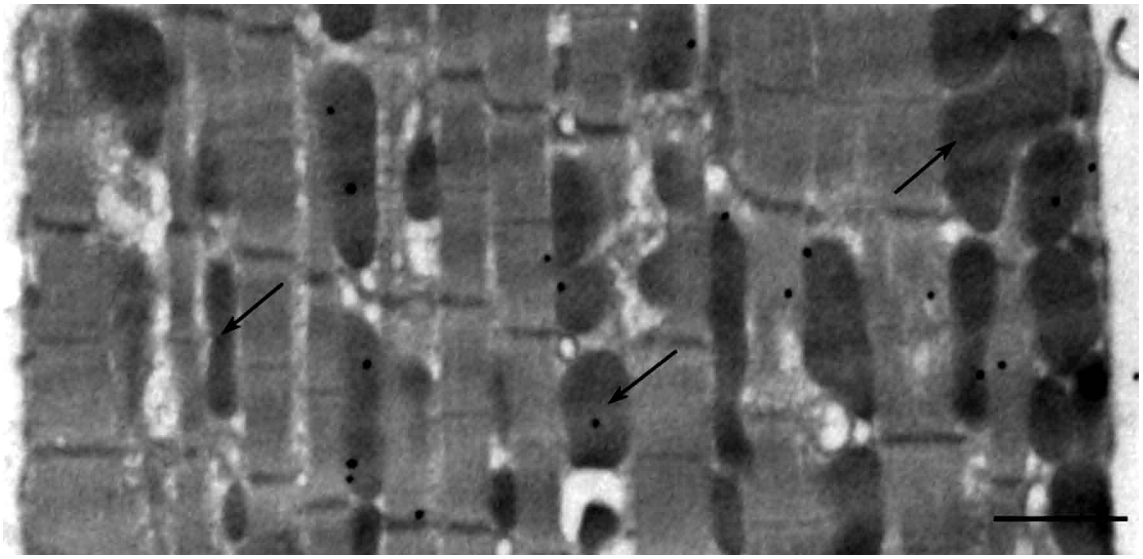

Figure 7. Control specimen in EM. Cells from the left ventricle were treated by primary antibodies mixed with the antigen prior to labelling. *Arrows* – mitochondria. *Bar*: 1 μm

in the previous studies was inconsistent and mostly at the level of background.

The presence of immunogold in sarcoplasmic reticulum and myofibrils at different levels of the sarcomere shows a similar pattern of distribution as demonstrated already in our previous publications (Maco et al. 2000, 2001).

Additional work is necessary to clarify the functional significance of S100A1 in mitochondria and identify corresponding target proteins and signalling cascades playing a role at this cellular level. Recently, Boerries et al. (2007) have demonstrated an interaction of S100A1 with the mitochondrial F_1-ATPase, which affects F_1-ATPase activity and cellular ATP production.

In a previous study on the rescue of failing myocardium following cardiac S100A1 gene delivery Most et al. (2004) have found that gene addition restored the depressed Pcr/ATP ratio to normal values and normalized impaired energy supply in failing cardiomyocytes.

The importance of mitochondria for Ca^{2+} homeostasis in cardiac muscle is well documented as exemplified recently by Seguchi et al. (2005), who identified mitochondria being responsible for differences in propagation of Ca^{2+} release between atrial and ventricular cardiac myocytes.

Acknowledgements. We like to thank Dr. G. E. Ackermann for critical reading. This work was supported by the Slovak Grant Agency for Science (VEGA Grant No. 2/5111/27), Slovak Science and Technology Assistance Agency (Grant APVV-51-027404) and the Swiss National Science Foundation.

References

Adhikari B. B., Wang K. (2001): S100A1 modulates skeletal muscle contraction by desensitizing calcium activation of isometric tension, stiffness and ATPase. FEBS Lett. **497**, 95–98

Arcuri C., Giambanco I., Bianchi R., Donato R. (2002): Annexin V, annexin VI, S100A1 and S100B in developing and adult avian skeletal muscles. Neuroscience **109**, 371–388

Boerries M., Most P., Gledhill J. R., Walker J. E., Katus H. A., Koch W. J., Aebi U., Schoenenberger C. A. (2007): The Ca^{2+}-dependent interaction of S100A1 with the F_1-ATPase leads to an increased ATP content in cardiomyocytes. Mol. Cell. Biol. **27**, 4365-4373

Brezová A., Uhrík B., Heizmann C. W. (2001): Immunolabelling on ultrathin cryosections in the study of subcellular localization of S100A1 in rat heart. Histochem. J. **33**, 471

Brezová A., Uhrík B., Heizmann C. W. (2002): Subcellular localization of S100A1 protein in normal rat heart obtained by immunolabeling of ultrathin cryosections. Physiol. Res. **51**, 4P

Donato R., Giambanco I., Aisa M. C., di Geronimo G., Ceccarelli P., Rambotti M. G., Spreca A. (1989): Cardiac S-100a0 protein: purification by a simple procedure and related immunocytochemical and immunochemical studies. Cell Calcium **10**, 81–92

Haimoto H., Kato K. (1987): $S100a_0$ ($\alpha\alpha$) protein, a calcium-binding protein, is localized in the slow-twitch muscle fiber. J. Neurochem. **48**, 917–923

Haimoto H., Kato K. (1988): S100a0 (alpha alpha) protein in cardiac muscle. Isolation from human cardiac muscle and ultrastructural localization. Eur. J. Biochem. **171**, 409–415

Heierhorst J., Kobe B., Feil S. C., Parker M. W., Benian G. M., Weiss K. R., Kemp B. E. (1996): Ca^{2+}/S100 regulation of giant protein kinases. Nature **380**, 636–639

Heizmann C. W., Ackermann G. E., Galichet A. (2007): Pathologies involving the S100 proteins and RAGE. In: Calcium Signalling and Disease. Molecular pathology of calcium (Eds. E. Carafoli and M. Brini), Springer (in press)

Ilg E. C., Schäfer B. W., Heizmann C. W. (1996): Expression pattern of S100 calcium-binding proteins in human tumors. Int. J. Cancer **68**, 325–332

Ivanenkov V. V., Dimlich R. V. W., Jamieson G. A. Jr. (1996): Interaction of S100a0 protein with the actin capping protein, CapZ: Characterization of a putative S100a0 binding site in CapZa-subunit. Biochem. Biophys. Res. Commun. **221**, 46–50

Kiewitz R., Acklin C., Schäfer B. W., Maco B., Uhrík B., Wuytack F., Erne P., Heizmann C. W. (2003): Ca^{2+}-dependent interaction of S100A1 with the sarcoplasmic reticulum Ca^{2+}-ATPase2a and phospholamban in the human heart. Biochem. Biophys. Res. Commun. **306**, 550–557

Lah J. J., Hayes D. M., Burry R. W. (1990): A neutral pH silver development method for the visualization of 1-nanometer gold particles in pre-embedding electron microscopic immunochemistry. J. Histochem. Cytochem. **38**, 503–508

Maco B., Uhrík B., Heizmann C. W. (2000): Distribution of the Ca^{2+}-binding S100A1 protein at different sarcomere lengths of slow and fast rat skeletal muscles. Gen. Physiol. Biophys. **19**, 237–244

Maco B., Mandinova A., Dürrenberger M., Schäfer B. W., Uhrík B., Heizmann C. W. (2001): Ultrastructural distribution of the S100A1 Ca^{2+}-binding protein in the human heart. Physiol. Res. **50**, 567–574

Mandinova A., Atar D., Schäfer B. W., Spiess M., Aebi U., Heizmann C. W. (1998): Distinct subcellular localization of calcium binding S100 proteins in human smooth muscle cells and their relocation in response to rises in intracellular calcium. J. Cell Sci. **111**, 2043–2054

Marenholz I., Heizmann C. W., Fritz G. (2004): S100 proteins in mouse and man: from evolution to function and pathology (including an update of the nomenclature). Biochem. Biophys. Res. Commun. **322**, 1111–1122

Most P., Pleger S. T., Volkers M., Heidt B., Boerries M., Weichenhan D., Loffler E., Janssen P. M., Eckhart A. D., Martini J., Williams M. L., Katus H. A., Remppis A., Koch W. J. (2004): Cardiac adenoviral S100A1 gene delivery rescues failing myocardium. J. Clin. Invest. **114**, 1550–1563

Most P., Boerries M., Eicher C., Schweda C., Volkers M., Wedel T., Sollner S., Katus H. A., Remppis A., Aebi U., Koch W. J., Schoenenberger C. A. (2005): Distinct subcellular location of the Ca^{2+}-binding protein S100A1 differentially modulates Ca^{2+}-cycling in ventricular rat cardiomyocytes. J. Cell Sci. **118**, 421–431

Seguchi H., Ritter M., Shizukuishi M., Ishida H., Chokoh G., Nakazawa H., Spitzer K. W., Barry W. H. (2005): Propagation of Ca^{2+} release in cardiac myocytes: role of mitochondria. Cell Calcium **38**, 1–9

Tokuyasu K. T. (1986): Application of cryoultramicrotomy to immunocytochemistry. J. Microsc. **143**, 139–149

Treves S., Scutari E., Robert M., Groh S., Ottolia M., Prestipino G., Ronjat M., Zorzato F. (1997): Interaction of S100A1 with the Ca^{2+} release channel (ryanodine receptor) of skeletal muscle. Biochemistry (USA) **36**, 11496–11503

Yamasaki R., Berri M., Wu Y., Trombitas K., McNabb M., Kellermayer M. S., Witt C., Labeit D., Labeit S., Greaser M., Granzier H. (2001): Titin-actin interaction in mouse myocardium: passive tension modulation and its regulation by calcium/S100A1. Biophys J. **81**, 2297–2313

Final version accepted: March 20, 2007